Croll Revisited:

Why is the Northern Hemisphere Warmer than the Southern Hemisphere?

Sarah M. Kang *

School of Urban and Environmental Engineering

Ulsan National Institute of Science and Technology, Ulsan, Republic of Korea

Richard Seager

Lamont Doherty Earth Observatory

Columbia University, Palisades, New York

Date of Initial Submission: Mar 31, 2011

Date of Revision: Dec 01, 2011

Date of Rejection: Apr 05, 2012

* *Corresponding author address:* Sarah M. Kang, 100 Banyeon-ri, Eonyang-eup, Ulju-gun, Ulsan, Korea 698-798. E-mail: skang@unist.ac.kr

ABSTRACT

The question of why, in the annual-mean, the Northern Hemisphere is warmer than the Southern Hemisphere is addressed, revisiting an 1870 paper by James Croll. We first show that ocean is warmer than land in general which, acting alone, would make the Southern Hemisphere with greater ocean fraction warmer. Croll thought it was caused by greater specific humidity and greenhouse trapping over ocean than over land. However, for any given temperature, greenhouse trapping is actually greater over land. Instead, oceans are warmer than land because of smaller surface albedo. However, inter-hemispheric differences in total albedo are negligible because the impact of differences in land-sea fraction are offset by Southern Hemisphere ocean and land reflecting more than their Northern Hemisphere counterparts. In agreement with Croll, it is shown that northward cross-equatorial ocean heat transport is critical for the warmer Northern Hemisphere. This is examined in a simple box model based on the energy budget of each hemisphere. The inter-hemispheric difference forced by ocean heat transport is enhanced by the positive water vapor-greenhouse feedback, and is partly compensated by the southward atmospheric energy transport. To fully explain the temperature difference in this way, requires a northward ocean heat transport at the extreme of observational estimates. A better fit to data is found when a larger basic state greenhouse trapping in the Northern Hemisphere, conceived as imposed by continental geometry, is imposed. Therefore, despite some modifications to his theory, analysis of modern data confirms Croll's 140 year-old theory that the warmer Northern Hemisphere is partly because of northward cross-equatorial ocean heat transport.

1. Introduction

One of the most fundamental features of the Earth's climate is that the Northern Hemisphere (NH) is warmer than the Southern Hemisphere (SH) (Fig. 1). There are several possible reasons for this. An informal poll of members of the public and some scientists often produces the answer that it is because the NH has more land and, therefore, heats up more in summer because of the lesser heat capacity. On the other hand, many scientists argue that it is because the ocean transports heat northward across the equator. We have also encountered more subtle arguments such as continental geometry that results in upwelling and equatorward sea ice export in the Antarctic Circumpolar Current (ACC) and Southern Ocean (SO) cooling the SH. Also, it could be argued that the impact of continental geometry on subtropical coastal upwelling preferentially cools the south (Philander et al. 1996). Finally, it could be a transient response to greenhouse gas forcing because the NH has the larger land fraction and heats up faster than the more oceanic SH. While the inter-hemispheric temperature asymmetry is interesting in and of itself, it is also of practical importance because of the influence it exerts on the position of the Intertropical Convergence Zone (ITCZ) (Kang et al. 2008) whose rains are relied upon by many tropical societies for their water and food production.

Although it still seems unclear exactly why the NH is warmer than the SH, James Croll, the founder of the astronomical theory of the ice ages, provided an explanation as early as 1870 (Croll 1870). He thought that the hemisphere with more ocean should be warmer than the one with more land because of higher atmospheric specific humidity, and hence, more greenhouse trapping. Interestingly, we will show that this is in fact incorrect: the

greenhouse trapping in general is greater over land than over ocean at the same temperature. Nonetheless, given that he thought that this mechanism would make the SH warmer than the NH, Croll claimed that the NH was actually warmer because the ocean transports heat northward across the equator:

> The lower mean temperature of the southern hemisphere is due to the amount of heat transferred over from that hemisphere to the northern by ocean-currents.

Croll′s arguments for how currents accomplish this transport was stated as follows:

> Since there is a constant flow of water from the southern hemisphere to the northern in the form of surface currents, it must be compensated by undercurrents of equal magnitude from the northern hemisphere to the southern. The currents, however, which cross the equator are far higher in temperature than their compensating undercurrents; consequently there is constant transference of heat from the southern hemisphere to the northern.

He argues that this idea is supported by the fact that the tropical oceans are cooler than the tropical land as a result of the huge ocean heat flux divergence. While Croll was correct that ocean heat flux divergence does cool some equatorial ocean regions, averaged over longitude it turns out that the tropical oceans are warmer than the tropical land masses. Nevertheless, Croll′s northward cross-equatorial ocean heat transport (OHT) explanation is probably the dominant one amongst scientists (e.g. Toggweiler and Bjornsson 2000, the existence of a southward flowing deep western boundary current in the tropical North Atlantic is shown in, for example, Molinari et al. 1992). It is truly remarkable that in 1870, Croll 1) knew that the NH was warmer than the SH, 2) was able to infer a cross-equatorial OHT and 3) provided

a coherent explanation for the temperature asymmetry that, though largely forgotten, is still invoked 140 years later. As we will show here, Croll appears to have been correct.

2. Data

For surface temperature, NCEP/NCAR reanalysis data (Kistler and Coauthors 2001) for the period from 1979 to 2010 are used. The NCEP/NCAR reanalysis data has equally spaced 192 longitudinal points and unequally spaced 94 latitudinal points. As reanalysis data might not be the best for inferring surface temperature as it is a derived quantity based on the energy balance over land, we have also used observed surface air temperatures in Jones et al. (1999) for the period of 1850 and 2010. The data has a horizontal resolution of 5° longitude × 5° latitude. We have fully confirmed that the results in association with surface air temperature data is consistent between the two data sets. Hence, the figures are shown only using the higher resolution NCEP/NCAR reanalysis data for simplicity and the values in the text show the mean and the standard deviation from the two data sets for 1979–2010. The annual mean as well as seasonal averages will be analyzed where winter (summer) in the NH is computed as the average of December-to-February (June-to-August) and vice versa in the SH.

To understand the inter-hemispheric differences in surface temperature, the radiation budget and the meridional energy transport by the atmosphere and ocean will be examined. The top-of-atmosphere (TOA) energy budget is determined by satellite data from the Clouds and the Earth's Radiant Energy System (CERES; Wielicki et al. 1996), which is on a T63 Gaussian grid, for March 2000 through October 2005 after some adjustments are made as

described in Fasullo and Trenberth (2008a). The atmospheric energy transport – the vertical integral of the meridional transport of the sensible heat, potential energy, kinetic energy, and latent energy – is computed from NCEP/NCAR (Kistler and Coauthors 2001) and ERA40 (Uppala and Coauthors 2005) reanalyses data for 1979–2007, and the adjusted data using the two reanalyses is obtained from Fasullo and Trenberth (2008b). For the oceanic energy transport, due to large uncertainties in the ocean data, we consider a range of values as discussed in Section 4a. The total cloud amount in Section 4b is from the International Satellite Cloud Climatology Project (ISCCP) cloud product (Rossow and Schiffer 1991), of which resolution is 2.5° longitude × 2.5° latitude, for the period from July 1983 to June 1991. Although the periods covered by each data set vary widely, the inter-hemispheric temperature contrast from NCEP/NCAR, which is the focus of this study, for the four different periods given above does not vary much, with the NH warmer by 1.24°C on average with 0.09°C standard deviation. This justifies the use of radiation budget for the available period to understand the mean inter-hemispheric temperature contrast. The inter-hemispheric temperature difference in the two data sets as a function of time is shown and discussed in the Appendix.

3. Temperature Differences

a. Inter-hemispheric Differences

The NH is warmer than the SH by 1.24±0.16°C in the annual mean (Fig. 1a). The warmer NH is also found in the multi-model mean of the preindustrial runs of 24 CMIP3 models

(Meehl et al. 2007), but with a smaller magnitude of 1.13°C. This suggests that the warmer NH is not a transient adjustment to greenhouse gas forcing with the more-land hemisphere leading, rather it is a basic characteristic of the Earth's climate. This is consistent with Croll identifying the inter-hemispheric temperature difference in 1870 before human impacts on the global scale climate system were appreciable. Interestingly, not all models produce a warmer NH, but the details are beyond the scope of the paper. Furthermore, the inter-hemispheric difference is also present at 700mb with the NH 2.0°C warmer than the SH, excluding the possibility of the surface temperature difference being caused by Antarctica′s high elevation.

When divided into seasons, that is, NH summer compared to SH summer and NH winter compared to SH winter, it is clear that the warmer NH in the annual mean results from the inter-hemispheric north minus south difference in summers of 4.35±0.21°C being partly offset by a smaller, opposite sign, difference of 2.20±0.42°C in winters. There is also a greater seasonal variation of temperature in the NH, 11.70±0.42°C, as opposed to 5.10±0.14°C in the SH, because the massive NH continents have interiors far from the oceans that warm in summer and cool in winter whereas SH continents are more influenced by ocean temperatures that themselves vary less with season due to large thermal inertia and storage of heat within the wind-driven mixed layer.

As land and ocean temperatures are vastly different due to contrasting thermal inertia and heat storage, it is useful to breakdown the inter-hemispheric temperature difference as following:

$$\Delta T = f_{O,N}T_{O,N} + (1 - f_{O,N})T_{L,N} - f_{O,S}T_{O,S} - (1 - f_{O,S})T_{L,S}. \quad (1)$$

Here, ΔT denotes the difference of temperature between the two hemispheres, f_O is fraction of ocean, T_L is area-weighted average temperature of land and T_O area-weighted ocean temperature. The subscripts N and S denote the northern and the southern hemispheres, respectively. The hemispheric mean temperatures of ocean and land, T_O and T_L, for both hemispheres are compared separately in Figs. 1b and 1c. The NH is warmer than the SH over ocean in both seasons and over land in summer. The latitudinal structure of the NH–SH difference in T_O in Fig. 2b indicates that the NH oceans are warmer than the SH oceans throughout the year at almost all latitudes. NH land is warmer than SH land in summer (Fig. 2c). However, between the latitudes of 28° and 66° where the vast northern continents are, winter T_L is cooler in the north than the south because the southern continental temperatures are more moderated by ocean temperatures. At these latitudes, summer T_L is warmer in the NH by 1.45±0.35°C but winter T_L is colder by 3.35±0.63°C. This implies the cooling effect of land in winter outweighs its warming effect in summer. Hence, in the annual mean the presence of the NH midlatitude continents tends to actually cool the NH relative to the SH, as evidenced by colder northern extratropics than the southern extratropics (Fig. 2a). However, the tropical land regions equatorward of 28° and the high latitudes poleward of 66° are warmer in the north almost throughout the year.

As depicted in Fig. 3, the differences in land (or ocean) fraction between the two hemispheres complicates the picture of dividing hemispheric mean temperature into contributions from T_L and T_O. Because there is a larger ocean fraction in the south, ocean temperatures are weighted more when computing the hemispheric mean. For example, during winters, although NH oceans are warmer than SH oceans, and the difference in land temperatures is small, the NH is colder than the SH because the land is colder than the ocean and the

north has more land. Hence, in addition to temperature differences between land and ocean, both within a hemisphere and between the hemispheres, the inter-hemispheric temperature difference is also contributed by differences in the fractional coverage of ocean. Therefore, we divide up the inter-hemispheric difference into these three components. Eq. (1) is rewritten as:

$$\Delta T = f_{O,N}(T_{O,N} - T_{O,S}) + (1 - f_{O,S})(T_{L,N} - T_{L,S}) + (f_{O,S} - f_{O,N})(T_{L,N} - T_{O,S}). \quad (2)$$

These three terms can be thought of as, in order, a term due to differences in ocean temperature, second, a term due to differences in land temperature and, third, a term due to differences in land and ocean fractions. Fig. 4 shows the decomposition of inter-hemispheric temperature differences using Eq. (2) for the annual mean and each season. The warmer NH in the annual mean is due to both the ocean and land being warmer in the north than the south while this is partly offset by the larger fraction of land in the north which tends to make the NH cooler. As seen from Fig. 2, the greater land fraction in the NH warms northern summers, but greatly cools winters and hence cools the NH in the annual mean. In all seasons, the warmer ocean in the north contributes the most to preferentially warming the NH.

b. Ocean versus Land Temperatures

It is shown in the last section that land, compared to ocean, gets colder in winter by a larger amount than it gets warmer in summer, suggesting the hemisphere with the larger land fraction should be colder on average: this effect would make the SH warmer than the NH. Here, we examine, and explain why, in general, ocean is warmer than land. Fig. 5a shows the

latitudinal distribution of the difference between the ocean and land temperatures. In winter, T_O is significantly warmer than T_L at all latitudes because land with small heat capacity cools more effectively than the ocean. In contrast, in summer, T_L is warmer than T_O in the mid- to high latitudes because the land warms up more than the ocean. This seasonal variation is greater in the north because the northern continents are larger and more shielded from the mitigating ocean effects. As expected, there is little seasonal variation in the tropics, with the ocean always being warmer than the land. Because the degree to which the ocean is warmer in winter is much larger than the degree to which ocean is colder in summer, ocean in the annual mean is warmer than land at every latitude. If this was the only process operating then we would expect the SH, with more ocean, to be warmer than the NH. Or, as Croll stated it:

> Were there no ocean-currents, it would follow, according to theory, that the southern hemisphere should be warmer than the northern, because the proportion of sea to land is greater on that hemisphere than on the northern; but we find that the reverse is the case.

Then, why is ocean warmer than land in general? Croll (1870) thought that the ocean will be warmer because of the greater amount of water vapor above and larger greenhouse trapping, (although he did not use that term). Croll argued that:

> The aqueous vapour of the air acts as a screen to prevent the loss by radiation from water, while it allows radiation from the ground to pass more freely into space; the atmosphere over the ocean consequently throws back a greater amount of heat than is thrown back by the atmosphere over land.

To check this, the greenhouse trapping, G, is computed as the difference between the upward longwave radiation at the surface and the outgoing longwave radiation (OLR), that is,

$$G \equiv \epsilon\sigma T^4 - F \tag{3}$$

where ϵ is surface emissivity, σ is Stefan-Boltzmann constant, T is surface temperature, and F is OLR from CERES. The entire upward longwave flux at the surface, $\epsilon\sigma T^4$ is obtained from Fasullo and Trenberth (2008a). The latitudinal difference of G over ocean and land in Fig. 5b indeed indicates that, at a given latitude, the greenhouse trapping is generally larger over the ocean in the annual mean. The exception is over the lower latitudes in the SH and arises from a contrast between large greenhouse trapping over the Amazon and Congo and weak trapping over the cool southeast tropical Pacific and Atlantic Oceans (refer to Fig. 12). However, G_O could be larger than G_L solely because T_O is warmer than T_L. Hence it is more informative to compare G over ocean and land at the same temperature. To do so, the global temperature data is binned in intervals of 2°C, and G, multiplied by the grid area, is summed within the bin. Fig. 6 indicates that the greenhouse trapping is in fact larger for any given temperature over the land than over the ocean. The exceptions are at very high temperatures where there is very high greenhouse trapping over the Indo-Pacific warm pool and at very low temperatures where there is very weak trapping over very cold and dry continents. Over land, the atmospheric specific humidity can get very high within summer monsoons, especially over Asia and North America. In contrast, over oceans, the atmospheric specific humidity can get very low in the descending, eastern, branches of the subtropical anticyclones, which partly owe their existence to monsoonal heating during summer over land (Rodwell and Hoskins 2001; Seager et al. 2003). Hence, greater greenhouse trapping

over the ocean cannot be the reason why the ocean is warmer than the land. The reason for the ocean being warmer than land is instead because of the smaller TOA albedo over ocean (Fig. 5c).

Do inter-hemipsheric TOA albedo differences then contribute to the inter-hemispheric temperature difference with the Southern Hemisphere having a lower albedo? Following Eq. (2), the north-south difference of shortwave reflection at TOA ($S^{\uparrow}$) from CERES can be decomposed as:

$$\Delta S^{\uparrow} = f_{O,N}(S^{\uparrow}_{O,N} - S^{\uparrow}_{O,S}) + (1 - f_{O,S})(S^{\uparrow}_{L,N} - S^{\uparrow}_{L,S}) + (f_{O,S} - f_{O,N})(S^{\uparrow}_{L,N} - S^{\uparrow}_{O,S}).$$

The inter-hemispheric difference of $S^{\uparrow}$ resulting from its differences over ocean, those over land, and land-ocean fraction difference is plotted in Fig. 7. More ocean cover in the SH indeed acts to decrease $S^{\uparrow}$ in the SH compared to the NH. However this difference is offset by the fact that the Southern Hemisphere ocean and land reflect more than their Northern Hemisphere counterparts. This is partly because of more clouds in the SH (refer to Fig. 11) due to both extensive subtropical stratus decks and cloud cover over the Southern Ocean. Hence, the hemispheric mean difference in shortwave reflection at TOA is only 0.2 Wm^{-2}, suggesting little impact of $\Delta S^{\uparrow}$, or, equivalently the inter-hemispheric difference of TOA albedo on the inter-hemispheric temperature difference.

4. Meridional Energy Transport and Radiation Budget

Regional temperatures are determined by the radiation budget and the energy transports by the atmosphere and ocean. One may expect warmer temperature where there is more

greenhouse trapping, less shortwave reflection, and more energy convergence by atmosphere and ocean. Hence, in this section, the top-of-atmosphere (TOA) radiation budget and meridional energy transports by ocean and atmosphere are examined to study what leads to the warmer NH.

a. Cross-equatorial Oceanic Energy Transports

The oceanic energy transport divergence is balanced by the ocean heat content tendency and the downward surface fluxes over the ocean, which in turn is determined by the atmospheric energy transport divergence and tendency and the net TOA radiative flux. In Trenberth and Fasullo (2008), TOA flux is determined by satellite retrievals from ERBE and CERES and atmospheric energy transport divergence is computed from reanalyses. Trenberth and Fasullo (2008) used three different ocean data sets to estimate the ocean heat content tendency. By combining the ERBE and CERES data with atmospheric heat transports calculated with different reanalysis, and the three different estimates of ocean heat tendency, Trenberth and Fasullo (2008) were able to create nine estimates of the ocean heat transport providing for a median estimate with two standard deviation error bars.

In the Atlantic, they found the median gave a large northward cross-equatorial ocean transport of 0.56±0.09 PW in the annual mean (Trenberth and Fasullo 2008). The yearlong northward transport corresponds to a warmer North Atlantic than the South Atlantic in all seasons (Fig. 8). In the Pacific, the median gave little cross-equatorial transport regardless of season, with -0.01±0.19 PW in the annual mean (Trenberth and Fasullo 2008), but the coastal upwelling in the southern subtropics, west of Chile (Philander et al. 1996) still allows

the South Pacific to be colder than the North Pacific. In the Indian Ocean, there is a large seasonal cycle in the cross-equatorial ocean transport, with the median of the estimates having 1.4PW to the north in boreal winter (December through February) and 1.8PW to the south in austral winter (June through September) (Loschnigg and Webster 2000). Hence, when comparing NH winter with SH winter, and vice versa, Indian OHT has little impact on the inter-hemispheric temperature contrast.

Because of the large seasonality in the Indian sector, the total energy transport by the ocean also exhibits a pronounced seasonal variability with a northward transport in boreal winter and a southward transport in boreal summer (Fig. 9a in Trenberth and Fasullo 2008). However, in the annual mean, the total cross-equatorial ocean transport is small with the median estimate providing $0.1PW$ with a two standard deviation spread of 0.6PW. However, the fact that warmer ocean temperatures in the north are most responsible for the warmer NH (Fig. 4), and that the Atlantic sector exhibits the largest inter-hemispheric contrast (Fig. 8) clearly do hint at the important role of cross-equatorial ocean transport although, clearly, the quality of ocean data is insufficient to support this assertion. Nonetheless, the simple box model calculation in Section 5 suggests that the OHT must be northward across the equator and within the error bars of the estimates of Trenberth and Fasullo (2008).

b. TOA Radiation Budget

The inter-hemispheric differences of downward and upward shortwave radiation at TOA, and greenhouse trapping are shown in Fig. 9. The SH receives 0.67 Wm^{-2} more incoming solar radiation at TOA than the NH because the Earth is closest to the Sun in SH summer.

This is partly offset by 0.20 Wm^{-2} more shortwave reflection at TOA in the SH than the NH in the annual mean. Hence, the net TOA solar radiation would tend to make the SH the warmer hemisphere but this effect is small. In contrast, there is a significantly larger amount, 5.67 Wm^{-2}, of longwave radiation trapped within the atmosphere in the NH in the annual mean. The seasonal variation of the NH minus SH difference in the greenhouse effect, positive in summer and negative in winter, is proportional to the inter-hemispheric temperature difference indicating the expected coupling between temperature and greenhouse trapping.

The latitudinal structures of the inter-hemispheric differences in upward TOA shortwave radiation and greenhouse trapping are shown in Fig. 10 and that of cloud cover in Fig. 11. In summer seasons, the NH reflects less shortwave radiation at TOA than the SH in the mid- to high latitudes. This is despite ice-free land albedo being larger than ocean albedo and is due to less cloud cover (Fig. 11) and the high albedo Antarctic ice sheet. In winter seasons, the NH reflects more partly due to snow cover over land poleward of 40°. However there is also more TOA shortwave reflection in the NH between 15° and 40° even though cloud cover is less in the NH all year long (Fig. 11). The TOA shortwave reflection is larger in the NH equatorward of 15° because of clouds associated with the NH ITCZ.

The gross features of the latitudinal structure in the inter-hemispheric difference in greenhouse trapping (Fig. 10) are well correlated with those in surface temperatures (Fig. 2a), except the local maxima in the deep tropics where there is little temperature differences. The peak in greenhouse trapping in the tropics is due to a super greenhouse effect, whereby greenhouse trapping increases with surface temperature so strongly that OLR actually decreases as the surface warms (Raval and Ramanathan 1989). During winter seasons the

smaller greenhouse trapping in the NH in the mid- to high latitudes is due to drying and cooling of the continents. The opposite occurs in summer seasons. The map of annual mean greenhouse trapping overlain with surface temperature (Fig. 12) clearly indicates that these are well correlated.

On the face of it then the NH is warmer than the SH because of the greater greenhouse trapping in the NH. This is in contrast with Croll′s expectation that the hemisphere with more ocean would have the greater trapping and be warmer were it not for ocean heat export from the SH to the NH. However it could be that the greater greenhouse trapping in the NH is not the cause of that hemisphere being warmer but a consequence, via the positive water vapor-greenhouse feedback, of the ocean heat export warming the NH relative to the SH.

5. A Simple Model of Inter-hemispheric Temperature Asymmetry

To examine whether inter-hemispheric differences in G are causes or effects of inter-hemispheric differences in surface T, a simple box model is used that solves for ΔT from the energy budget, as depicted in Fig. 13. The model conceptually follows those in Ramanathan and Collins (1991) and Sun and Liu (1996), except that the radiative budgets are not separated out into clear-sky and cloudy-sky regions and the subsurface ocean currents are not explicitly accounted for and instead ocean heat transport is specified. Two boxes with temperatures T_S and T_N respectively represent the SH and the NH. At TOA, there is net shortwave radiation S and outgoing longwave radiation F. For simplicity, the net

shortwave radiation S is considered to be the same for the two hemispheres by taking the global mean of S_0=239.5 Wm^{-2}. Since differences in S are small, taking the actual values for the respective hemisphere, S_S and S_N makes little difference. From Eq. (3), the OLR is given by $F = \sigma T^4 - G$ where σ=5.67$\times 10^{-8}$ $\mathrm{Wm}^{-2}\mathrm{K}^{-1}$, G is the greenhouse trapping and T is the surface temperature, T_S or T_N. The northward oceanic transport F_O is prescribed, but due to its uncertainties a range of values from 0 to 1.10 PW is used (Section 4a). The atmospheric transport F_A is thermally direct and parameterized as a function of $\Delta T = T_N - T_S$, i.e. $F_A = \frac{\partial F_A}{\partial \Delta T}\Delta T$. The annual mean values of F_A at the equator from Fasullo and Trenberth (2008b) and ΔT from NCEP/NCAR reanalysis are used between 1979 and 2007 to compute the coefficient, $\frac{\partial F_A}{\partial \Delta T}$, referred to as the strength of atmospheric transport, by regressing F_A onto ΔT. This yields the value of -0.20 PW K^{-1} with a correlation of 0.44 between the two time series which is significant at the 95% level. To express atmospheric and oceanic energy transport in a flux form in Wm^{-2}, F_A and F_O are divided by the hemispheric mean area, A_0. The energy budget for the two boxes can be written as:

$$S_0 - \sigma T_S^4 + G_S - F_O/A_0 + \left|\frac{\partial F_A/A_0}{\partial \Delta T}\right| \Delta T = 0 \tag{4}$$

$$S_0 - \sigma T_N^4 + G_N + F_O/A_0 - \left|\frac{\partial F_A/A_0}{\partial \Delta T}\right| \Delta T = 0 \tag{5}$$

The above equations can be linearized by applying the first-order Taylor expansion around global mean values denoted by the subscript 0 as:

$$S_0 - \{\sigma T_0^4 + 4\sigma T_0^3(T_S - T_0)\} + \{G_{0,S} + \frac{\partial G}{\partial T}(T_S - T_0)\} - F_O/A_0 + \left|\frac{\partial F_A/A_0}{\partial \Delta T}\right| \Delta T = 0 \tag{6}$$

$$S_0 - \{\sigma T_0^4 + 4\sigma T_0^3(T_N - T_0)\} + \{G_{0,N} + \frac{\partial G}{\partial T}(T_N - T_0)\} + F_O/A_0 - \left|\frac{\partial F_A/A_0}{\partial \Delta T}\right| \Delta T = 0 \tag{7}$$

Note that G is linearized at different basic states in each hemisphere ($G_{0,S}$ and $G_{0,N}$), in recognition of potential differences in thermal characteristics between the two hemispheres

not caused by the temperature difference but imposed by differences in fractional coverage of ocean, continental arrangements, etc. For example, $G_{0,N}$ could be larger than $G_{0,S}$, despite greater ocean fraction in the south, because subtropical dry regions over the ocean are more developed in the SH than the NH and due to massive humidity in Asia associated with the summer monsoon.

By adding the two equations, we get a constraint on the global mean greenhouse effect, $(G_{0,S}+G_{0,N})/2 = \sigma T_0^4 - S_0$ (=288.8 Wm^{-2}) where T_0 is the global-mean annual-mean surface temperature of 14.8°C. Eqs. (6) and (7) can be expressed in terms of one unknown, ΔT:

$$\left(2\sigma T_0^3 - \frac{1}{2}\frac{\partial G}{\partial T} + \left|\frac{\partial F_A/A_0}{\partial \Delta T}\right|\right)\Delta T = F_O/A_0 + \Delta G_0/2. \tag{8}$$

$\Delta G_0 \equiv G_{0,N} - G_{0,S}$ is the basic state G difference between the hemispheres. $\frac{\partial G}{\partial T}$ (=4.0 $\mathrm{Wm}^{-2}\mathrm{K}^{-1}$), referred to as the greenhouse trapping efficiency, is estimated as $4\sigma T_0^3 - \frac{\partial F}{\partial T}$ where $\frac{\partial F}{\partial T}$ (=−1.5 $\mathrm{Wm}^{-2}\mathrm{K}^{-1}$) is the regression coefficient relating the monthly anomalies of global mean OLR to that of T between 2001 and 2004 which are correlated with a coefficient of 0.40 significant at the 95% level. OLR is from CERES data and surface temperature T is from NCEP/NCAR reanalysis.

The model results for ΔT from Eq. (8) as a function of F_O for the case with ΔG_0=0 are plotted in Fig. 14a. The shading indicates the one standard deviation of observed ΔT from its global mean. The realistic solutions are those that fall within the shaded area. The reference state with the most reasonable estimates of parameters, $\frac{\partial G}{\partial T}$=4.0 $\mathrm{Wm}^{-2}\mathrm{K}^{-1}$ and $\frac{\partial F_A}{\partial \Delta T}$=0.20 $\mathrm{Wm}^{-2}\mathrm{K}^{-1}$, is plotted in black and requires large northward F_O of about 0.57 PW to fall in the realistic range of ΔT. When there is no cross-equatorial transport by the atmosphere (blue), ΔT increases and deviates from the realistic range for a cross-equatorial F_O greater

than 0.2PW, suggesting that the atmosphere acts to reduce the inter-hemispheric contrast. That is, with smaller $\frac{\partial F_A}{\partial \Delta T}$, the thermally direct F_A is smaller and the required magnitude of cross-equatorial F_O for yielding a reasonable ΔT is less. When the greenhouse trapping efficiency increases (red), the inter-hemispheric difference gets larger via positive water vapor feedback for a given F_O as the warmer NH gets even warmer and the cooler SH cools more. The resulting inter-hemispheric difference of greenhouse trapping, ΔG for a given ΔT is displayed in Fig. 14b. Here the horizontal shading shows the range of the observed ΔG. Because ΔG is determined by $\frac{\partial G}{\partial T}$ and ΔT, it changes only when the efficiency $\frac{\partial G}{\partial T}$ varies for a given ΔT and, hence, the lines representing cases with (black) and without (blue) atmosphere heat transport are overlapped. The greenhouse trapping contrast increases with larger ΔT or as its efficiency gets larger. In the cases with a realistic range of ΔT, the reference state including atmospheric energy transport yields ΔG that is at the margin of the observed range.

In the box model with the same basic state G in each hemisphere, the northward oceanic transport is the only mechanism that can produce a warmer NH. However, the magnitude of northward OHT needed for realistic solutions appears larger than the data supports (Section 4a). Hence, we consider the case with nonzero ΔG_0, since not all of ΔG in Fig. 9 need be a result of ΔT, but could be in part due to basic state differences as suggested in Fig. 6 and discussed above. The model solutions for F_O=0 as a function of ΔG_0 are shown in Figs. 14c and 14d. For the reference solution (black) to be in the realistic ΔT range, it requires $\Delta G_0 \approx$ 4 Wm^{-2}, which then yields $\Delta G \approx 9$ Wm^{-2}, much larger than the real value of 5.67 Wm^{-2}. *That is, with no ocean heat transport, too large of an inter-hemispheric difference of G is needed to obtain the right magnitude of* ΔT. We therefore consider a combination of the first

two models that takes into account both F_O and ΔG_0. Figs. 14e and 14f show the solutions for F_O=0.3 PW, which is within the range in Fasullo and Trenberth (2008b), as a function of ΔG_0. The realistic ΔT is obtained for $\Delta G_0 \approx 1.5$ Wm^{-2}, which then yields ΔG within the realistic range of about 6.0Wm^{-2}.

For plausible magnitudes of northward OHT, positive ΔG_0, greenhouse trapping efficiency and atmospheric heat transport strength, the box model does predict values of ΔT and ΔG that are consistent with those observed. Therefore the model supports the idea that a northward cross-equatorial OHT is required for the inter-hemispheric temperature difference on Earth, as Croll suggested.

6. Discussion

The box model based on the TOA energy budget suggests that the necessary factors for the NH to be warmer than the SH are:

- a northward cross-equatorial ocean heat transport
- a larger basic state greenhouse effect in the north

The larger annual-mean inter-hemispheric difference in the Atlantic sector (5.2°C) than in the Pacific sector (2.5°C) (Fig. 8) supports this idea because the northward cross-equatorial OHT occurs in the Atlantic Ocean (e.g. see Fig. 9 in Trenberth and Fasullo 2008). That is, the ocean transports energy northward, the NH gets warmer and this inter-hemispheric difference is enhanced by greenhouse trapping. Since the tropical mean atmospheric circulation is thermally direct, the inter-hemispheric temperature difference is partly compensated by the

atmospheric energy transport from the north to the south which is accomplished by having the mean ITCZ in the north (Kang et al. 2008, 2009).

However, the quality of ocean data is insufficient for deriving not only the magnitude but also the direction of cross-equatorial OHT. For the inter-hemispheric temperature difference to be entirely caused by northward cross-equatorial OHT a value ($\sim$0.6PW) at the very upper limit of the observational range is required. A more reasonable OHT is inferred if some portion of the inter-hemispheric temperature difference arises from a difference in the basic state greenhouse trapping, i.e. some aspect of the atmospheric circulation and humidity distribution that creates more greenhouse trapping in the NH than the SH independent of the temperature difference. However, since the greenhouse effect incorporates efficient positive feedback, it is difficult to extract this postulated basic state difference between the two hemispheres.

Only much more accurate OHT data, presumably obtained through combinations of in-situ data, atmospheric and oceanic Reanalyses, satellite data and adjoint methods, will be able to settle the contribution of cross-equatorial OHT to the inter-hemispheric temperature difference. The simple box model, solving for the energy balance of each hemisphere, aids understanding the cause for the warmer NH in a very straightforward manner. This simplicity is achieved by lumping together a number of factors such as clouds, topographic effects, continental distribution in aggregate form within the model parameters such as the basic state greenhouse trapping. As a consequence, we conclude that it is likely that there is an additional cause of the asymmetry in addition to cross-equatorial ocean heat transport but the simplicity of the model does not allow us to determine how this arises. The detailed mechanism as well as the issue of a postulated inter-hemispheric difference in basic state

greenhouse trapping would most likely be best addressed with idealized climate modeling. In the meantime the results presented here, including the results of the simple model do represent significant progress in understanding of this important aspect of the Earth's mean climate.

7. Conclusions

We have discussed why the NH is warmer than the SH in the annual mean and pursued the idea, put forth by Croll (1870), that it is caused by northward cross-equatorial OHT. Croll (1870) claimed that the hemisphere with the larger ocean fraction would be warmer because of higher specific humidity, and hence, more greenhouse trapping. It is true that the ocean is warmer than land at every latitude in the annual mean. However, we find that the greenhouse trapping is in fact larger over land than ocean at the same temperature. The reason for the warmer ocean is, instead, the smaller surface albedo of the ocean. Therefore the larger land fraction in the north acts to cool the NH relative to the SH. This effect is offset by the fact that both the NH land masses and the NH oceans are warmer than their SH counterparts.

Of these it is the warmer ocean in the north that contributes most to preferentially warming the NH. A simple box model based on the energy budget shows that in order to obtain an inter-hemispheric temperature difference within the observed range an unrealistically large greenhouse trapping difference is needed if there is no ocean transport across the equator. On the other hand, unrealistically large northward cross-equatorial ocean transport is needed for the case with no basic static greenhouse trapping difference between the

two hemispheres. The most reasonable solution combines a modest northward OHT and an inter-hemispheric difference in the basic state greenhouse trapping. Hence, the greater greenhouse trapping in the NH (by 5.7 Wm^{-2}) is not the main cause of the warmer north but more of a consequence, and the northward oceanic heat transport is critical to producing a warmer NH, consistent with Croll (1870). We also suggest that the inter-hemispheric temperature difference is contributed to by an inter-hemispheric difference in the basic state greenhouse trapping. This inter-hemispheric temperature difference created by these mechanisms is enhanced by the positive water vapor-greenhouse feedback. The thermally direct tropical mean atmospheric circulation then partly compensates for this inter-hemipsheric contrast by transporting energy southward in association with having the mean ITCZ in the NH.

It is normally assumed that the northward oceanic heat transport, which occurs in the Atlantic Ocean, is a result of the deep Atlantic meridional overturning circulation with northward surface flow, sinking in the North Atlantic and southward flow at depth (Molinari et al. 1992) and upwelling around Antarctica and it can be reproduced in this way easily in idealized models (Toggweiler and Bjornsson 2000). As such, it is a consequence of the arrangement of continents and oceans on the planet that enable the Atlantic Ocean to be saltier than the Pacific Ocean (Emile-Geay et al. 2003). On the other hand it has not to our knowledge been demonstrated that Atlantic cross-equatorial OHT could not exist in the absence of the deep overturning circulation just as it does (to the south) in the Indian Ocean. Consequently a definitive account of why the NH is warmer than the SH requires a thorough accounting for the causes of the cross-equatorial OHT because, as shown here, this is a fundamental cause of the asymmetry.

However, unless estimates of cross-equatorial OHT are highly inaccurate, it is unlikely that this is the sole cause of the inter-hemispheric temperature difference. An inter-hemispheric difference in greenhouse trapping appears to be a probable additional cause. This would likely be a result of how the arrangement of continents, and its impact on atmosphere-ocean circulation features such as monsoons, subtropical anticyclones and ocean upwelling regions, determines the distribution of atmospheric water vapor. To assess if this is so will require much more research including the use of idealized and comprehensive climate models.

The fact that the NH is warmer than the SH is potentially linked to the fact that the ITCZ is in the NH (Kang et al. 2008). The mechanisms for the inter-hemispheric temperature difference are such that we would expect the difference to change as a result of radiatively-forced climate change and, hence, influence the ITCZ position. For example, the hemispherically asymmetric anthropogenic aerosol distribution could impact the inter-hemispheric temperature contrast and, in turn, the ITCZ location both in the past and in the future (Cai et al. 2006). Millions of the world's population depend on ITCZ rains for their water and food making the problem of how ITCZ location is determined one of great social relevance. It is sobering that the current state of observations of the Earth's climate system is inadequate to fully answer such a fundamental question as why the NH is warmer than the SH and, hence provide a full account of why tropical rain belts are where they are.

APPENDIX

Fig. 15 compares the annual-mean inter-hemispheric temperature difference (ΔT) using the Jones et al. (1999) data and NCEP/NCAR reanalysis data. The two data sets show surpris-

ingly similar trend. ΔT was smaller in the mid 20^{th} century during the main period of high Northern Hemisphere aerosol concentrations until pollution controls and de-industrialization became effective at reducing emissions in the 1970's on. The Atlantic Multidecadal Oscillation (AMO) would also have contributed to a weaker difference in the the mid 20^{th} century but, as Mann and Emanuel (2006) claim, aerosol impacts and the AMO may not be entirely independent.

For the entire available period of each data set, ΔT=1.30±0.11 in the Jones et al. (1999) data and 1.27±0.17 in NCEP/NCAR. In particular, for the same period from 1979 to 2010, ΔT=1.34±0.15 in the Jones et al. (1999) data and 1.25±0.16 in NCEP/NCAR. Although the Jones et al. (1999) data exhibits slightly higher ΔT, the similarity of trends confirms the robustness. Hence, the figures are produced using finer resolution NCEP/NCAR, but the values in the text show the mean and the standard deviation from the two data sets.

Acknowledgments.

We thank David Battisti for useful discussions that initiated this work. Also, John Fasullo's help in interpreting the OHT data is greatly appreciated. RS was supported by NSF award ATM 08-04107.

REFERENCES

Cai, W., D. Bi, J. Church, T. Cowan, M. Dix, and L. Rotstayn, 2006: Pan-oceanic response to increasing anthropogenic aerosols: Impacts on the Southern Hemisphere oceanic circulation. *Geophys. Res. Lett.*, **33 (21)**.

Croll, J., 1870: XII. On Ocean-currents, Part I: Ocean-currents in relation to the Distribution of Heat over the Globe. *Philosophical Magazine and Journal of Science*, **39 (259)**, 81–106.

Emile-Geay, J., M. A. Cane, N. Naik, R. Seager, A. C. Clement, and A. van Geen, 2003: Warren revisited: Atmospheric freshwater fluxes and why is no deep water formed in the north pacific. *J. Geophys. Res.*, **108**, 3178.

Fasullo, J. T. and K. E. Trenberth, 2008a: The annual cycle of the energy budget. Part I: Global mean and land-ocean exchanges. *Journal of Climate*, **21 (10)**, 2297–2312.

Fasullo, J. T. and K. E. Trenberth, 2008b: The annual cycle of the energy budget. Part II: Meridional structures and poleward transports. *Journal of Climate*, **21 (10)**, 2313–2325.

Jones, P. D., M. New, D. E. Parker, S. Martin, and I. G. Rigor, 1999: Surface air temperature and its changes over the past 150 years. *Rev. Geophys.*, **37 (2)**, 173–199.

Kang, S. M., D. M. W. Frierson, and I. M. Held, 2009: The tropical response to extratropical thermal forcing in an idealized gcm: The importance of radiative feedbacks and convective parameterization. *Journal of the Atmospheric Sciences*, **66 (9)**, 2812–2827.

Kang, S. M., I. M. Held, D. M. W. Frierson, and M. Zhao, 2008: The response of the ITCZ to extratropical thermal forcing: Idealized slab-ocean experiments with a GCM. *Journal of Climate*, **21 (14)**, 3521–3532.

Kistler, R. and Coauthors, 2001: The NCEP–NCAR 50–Year Reanalysis: Monthly Means CD–ROM and Documentation. *Bull. Amer. Meteor. Soc.*, **82**, 247–267.

Loschnigg, J. and P. J. Webster, 2000: A Coupled Ocean–Atmosphere System of SST Modulation for the Indian Ocean. *J. Climate*, **13**, 3342–3360.

Mann, M. E. and K. A. Emanuel, 2006: Atlantic hurricane trends linked to climate change. *EOS*, **87 (24)**, 233–244.

Meehl, G. A., C. Covey, T. Delworth, M. Latif, B. McAvaney, J. F. B. Mitchell, R. J. Stouffer, and K. E. Taylor, 2007: The WCRP CMIP3 multimodel dataset. *Bull. Am. Meteorol. Soc.*, **88**, 1383–1394.

Molinari, R. L., R. A. Fine, and E. Johns, 1992: The deep western boundary current in the tropical north the deep western boundary current in the tropical north the deep western boundary current in the tropical north atlantic ocean. *Deep Sea Res.*, **39 (11/12)**, 1967–1984.

Philander, S. G. H., D. Gu, G. Lambert, T. Li, D. Halpern, N.-C. Lau, and R. C. Pacanowski, 1996: Why the ITCZ Is Mostly North of the Equator. *Journal of Climate*, **9 (12)**, 2958–2972.

Ramanathan, V. and W. Collins, 1991: Thermodynamic regulation of ocean warming by cirrus clouds deduced from observations of the 1987 El Niño. *Nature*, **351**, 27–32.

Raval, A. and V. Ramanathan, 1989: Observational determination of the greenhouse effect. *Nature*, **342**, 758–761.

Rodwell, M. J. and B. J. Hoskins, 2001: Subtropical anticyclones and summer monsoons. *J. Climate*, **14**, 3192–3211.

Rossow, W. B. and R. A. Schiffer, 1991: ISCCP cloud datasets. *Bull. Amer. Meteor. Soc.*, **72**, 2–20.

Seager, R., R. Murtugudde, N. Naik, A. Clement, N. Gordon, and J. Miller, 2003: Air–Sea Interaction and the Seasonal Cycle of the Subtropical Anticyclones*. *J. Climate*, **16**, 1948–1966.

Sun, D.-Z. and Z. Liu, 1996: Dynamic Ocean-Atmosphere Coupling: A Thermostat for the Tropics. *Science*, **272**, 1148–1150.

Toggweiler, J. R. and H. Bjornsson, 2000: Drake Passage and palaeoclimate. *Journal of Quaternary Science*, **15 (4)**, 1099–1417.

Trenberth, K. E. and J. T. Fasullo, 2008: An observational estimate of inferred ocean energy divergence. *Journal of Physical Oceanography*, **38 (5)**, 984–999.

Uppala, S. M. and Coauthors, 2005: The ERA-40 reanalysis. *Quart. J. Roy. Meteor. Soc.*, **131**, 2961–3012.

Wielicki, B. A., B. R. Barkstrom, E. F. Harrison, R. B. Lee, G. L. Smith, and J. E. Cooper, 1996: Clouds and the Earth's Radiant Energy System (CERES): An Earth Observing System experiment. *Bull. Amer. Meteor. Soc.*, **77**, 853–868.

List of Figures

6 The greenhouse trapping G (in W) for a given temperature T (in °C) over land (solid) and over ocean (dashed). 36

7 The annual mean inter-hemispheric difference of upward shortwave radiation at TOA ($\Delta S^{\uparrow}$), the fraction of $\Delta S^{\uparrow}$ resulting from the inter-hemispheric difference over ocean $f_{O,N}\Delta S^{\uparrow}_{O}$, over land $(1 - f_{O,S})\Delta S^{\uparrow}_{L}$, and from the inter-hemispheric difference in ocean fraction $(f_{O,S} - f_{O,N})(S^{\uparrow}_{L,N} - S^{\uparrow}_{O,S})$. Units are in Wm^{-2}. 37

8 The inter-hemispheric ocean temperature difference in the Atlantic (hatching), Pacific (dotted), and Indian (crossing) for each season. ΔT_O in the Pacific and the Atlantic are computed as the T_O difference between (0–60°N) and (60°S–0) at each basin, and in the Indian Ocean the difference is taken between (0–20°N) and (20°S–0). 38

9 The inter-hemispheric difference of downward shortwave radiation ($\Delta S^{\downarrow}$), upward shortwave radiation ($\Delta S^{\uparrow}$), and greenhouse trapping (ΔG) for annual mean (hatching), winter (dotted) and summer (crossing). Units are in Wm^{-2}. 39

10 The inter-hemispheric difference of (a) upward shortwave radiation ($\Delta S^{\uparrow}$), and (b) greenhouse trapping (ΔG) as a function of latitude for annual mean (thick solid), winter (thin dashed) and summer (thin dash-dot). Units are in Wm^{-2}. 40

11 The inter-hemispheric difference of cloud fraction with latitude for annual mean (thick solid), winter (thin dashed) and summer (thin dash-dot). 41

12 The global map of annual mean surface temperature (in °C) in black contour and greenhouse trapping (in Wm^{-2}) in color shading. The contour interval is 4°C and shading interval is 10 Wm^{-2}. 42

13 The schematic figure for the box model based on energy budget. The net incoming shortwave radiation S is balanced by outgoing longwave radiation F, meridional energy transports by atmosphere F_A and ocean F_O. The model solves for surface temperature T. The subscripts N and S denote the hemispheric mean in the north and the south, respectively. 43

14 Solutions from the box model: the inter-hemispheric difference of (a) surface temperature ($\Delta T = T_N - T_S$, in °C) as a function of prescribed oceanic transport F_O (in PW), and (b) greenhouse trapping ($\Delta G = G_N - G_S$, in Wm^{-2}) as a function of ΔT for the case with no basic state G difference (ΔG_0=0). (c,d) Same as (a,b) but as a function of $\Delta G_0 (= G_{0,N} - G_{0,S})$ for no oceanic transport (F_O=0). (e,f) Same as (c,d) but for the case with F_O=0.3PW. The reference state (black) is the solution with the most reasonable parameters, $\frac{\partial G}{\partial T}$=4.0$\mathrm{Wm}^{-2}\mathrm{K}^{-1}$ and $\frac{\partial F_A}{\partial \Delta T}$=0.20$\mathrm{Wm}^{-2}\mathrm{K}^{-1}$. Blue is the case with no cross-equatorial atmospheric heat transport $\frac{\partial F_A}{\partial \Delta T}$=0 and red is with stronger greenhouse trapping $\frac{\partial G}{\partial T}$=5.0$\mathrm{Wm}^{-2}\mathrm{K}^{-1}$. Black dashed lines denotes the annual mean values, and the gray shading denotes the one standard deviation of observed ΔT and ΔG. 44

15 The annual-mean inter-hemispheric temperature difference ($\Delta T = T_N - T_S$) in °C from 1850 to 2010 using the Jones et al. (1999) data (solid) and that from 1949 to 2010 using NCEP/NCAR reanalysis (dashed). 45

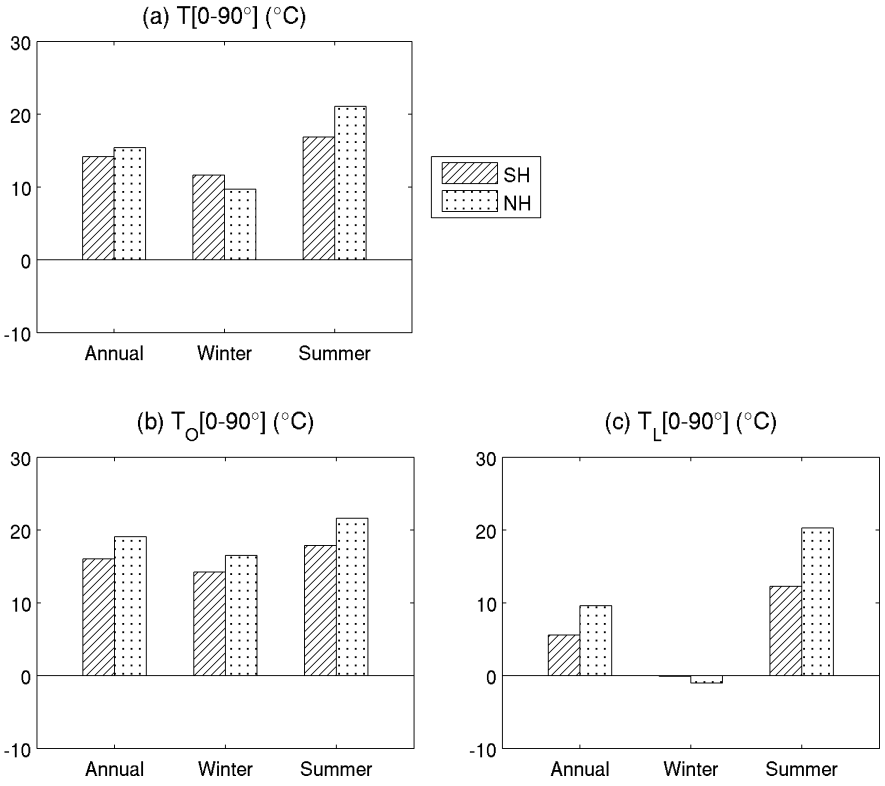

FIG. 1. The hemispheric mean (a) surface temperature, (b) ocean temperature, and (c) land temperature in the north (dotted) and the south (hatching) for annual mean, winter (DJF for the NH and JJA for the SH) and summer (JJA for the NH and DJF for the SH). Units are in °C.

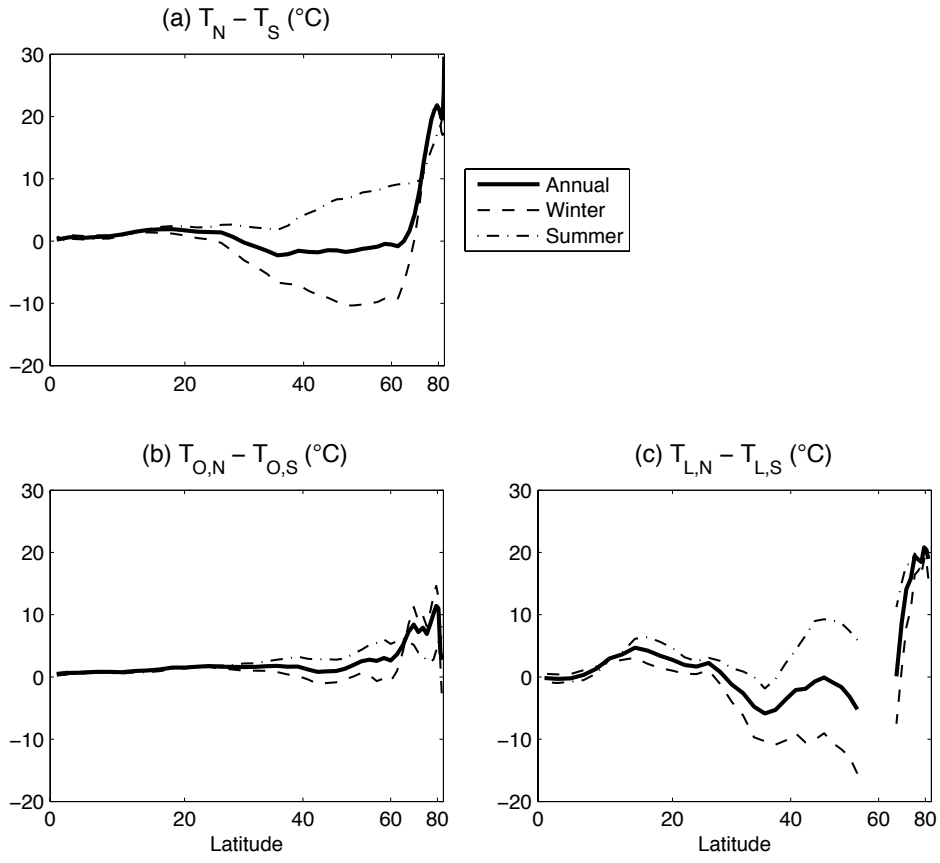

FIG. 2. The inter-hemispheric difference of (a) surface temperature, (b) ocean temperature, and (c) land temperature as a function of latitude for annual mean (thick solid), winter (thin dashed) and summer (thin dash-dot). Units are in °C. The x coordinate is linear in sine of latitude so that equal spacing corresponds to equal surface area on the globe.

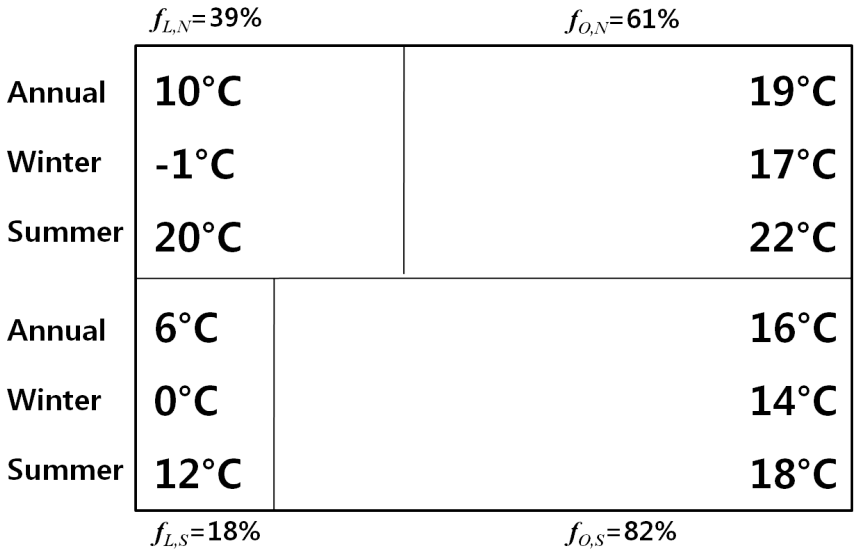

FIG. 3. The schematic figure of hemispheric mean temperatures of surface, ocean, and land for annual mean (green), winter (blue) and summer (red) and fractions of ocean (f_O) and land (f_L) cover.

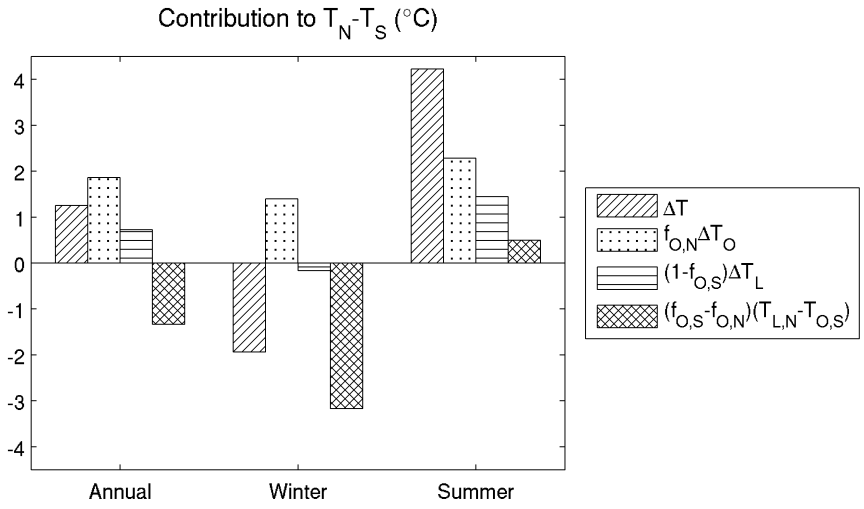

FIG. 4. The inter-hemispheric difference of surface temperature (hatching, ΔT), the fraction of ΔT resulting from differences in ocean temperatures (dotted), land temperatures (horizontal lines), and ocean fraction (crossing) for annual mean, winter and summer. Units are in °C.

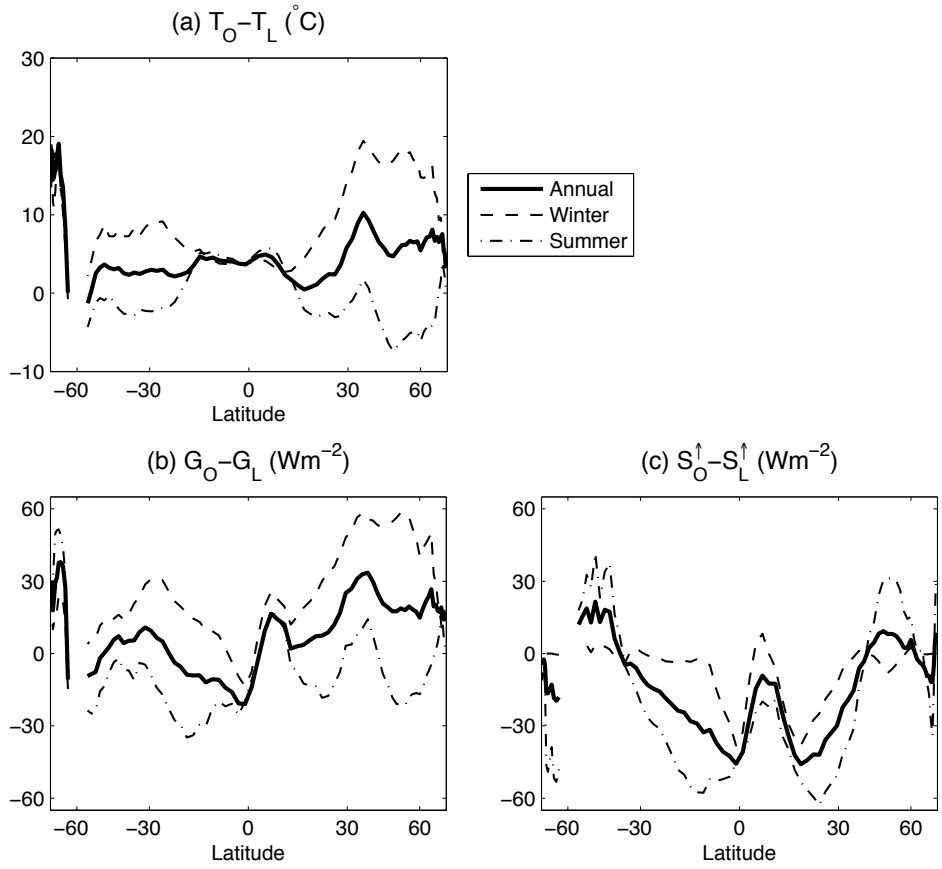

FIG. 5. The latitudinal difference between ocean and land of (a) temperatures T (in °C), (b) greenhouse trapping, G (in Wm^{-2}), and (c) upward shortwave radiation at TOA, $SW^{\uparrow}$ (in Wm^{-2}) for annual mean (thick solid), winter (thin dashed) and summer (thin dash-dot).

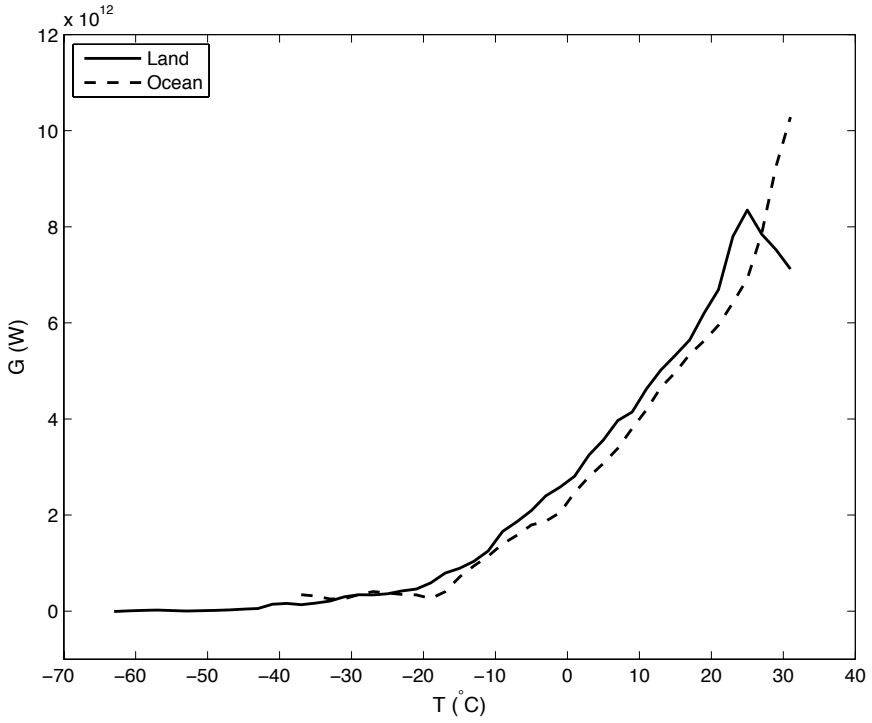

FIG. 6. The greenhouse trapping G (in W) for a given temperature T (in °C) over land (solid) and over ocean (dashed).

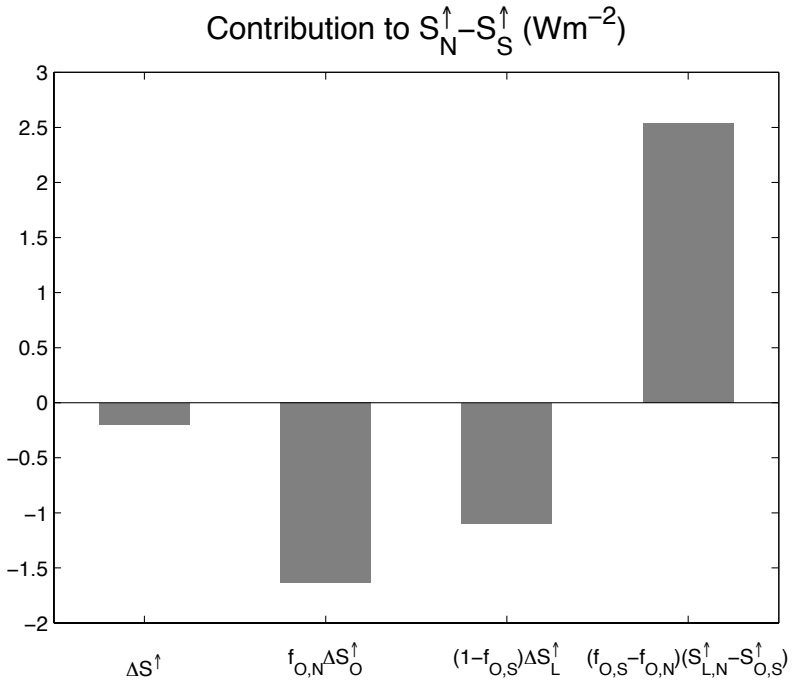

FIG. 7. The annual mean inter-hemispheric difference of upward shortwave radiation at TOA ($\Delta S^{\uparrow}$), the fraction of $\Delta S^{\uparrow}$ resulting from the inter-hemispheric difference over ocean $f_{O,N}\Delta S^{\uparrow}_O$, over land $(1 - f_{O,S})\Delta S^{\uparrow}_L$, and from the inter-hemispheric difference in ocean fraction $(f_{O,S} - f_{O,N})(S^{\uparrow}_{L,N} - S^{\uparrow}_{O,S})$. Units are in Wm^{-2}.

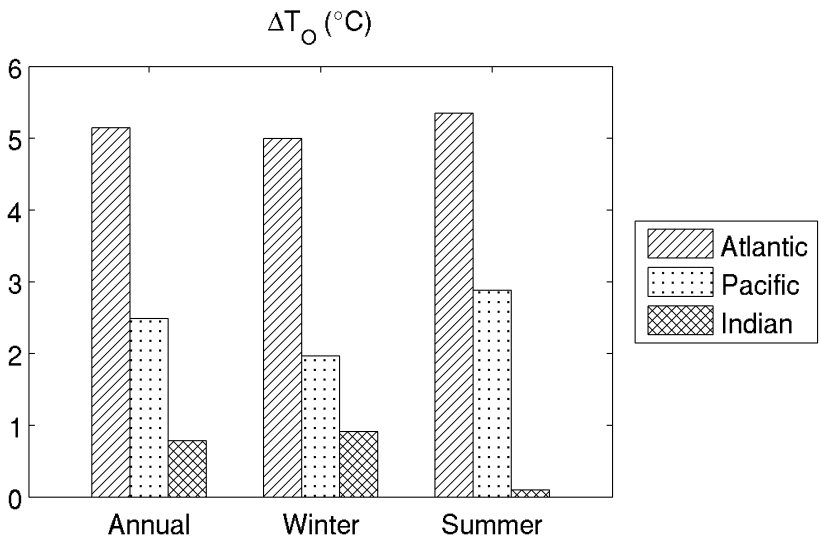

FIG. 8. The inter-hemispheric ocean temperature difference in the Atlantic (hatching), Pacific (dotted), and Indian (crossing) for each season. ΔT_O in the Pacific and the Atlantic are computed as the T_O difference between (0–60°N) and (60°S–0) at each basin, and in the Indian Ocean the difference is taken between (0–20°N) and (20°S–0).

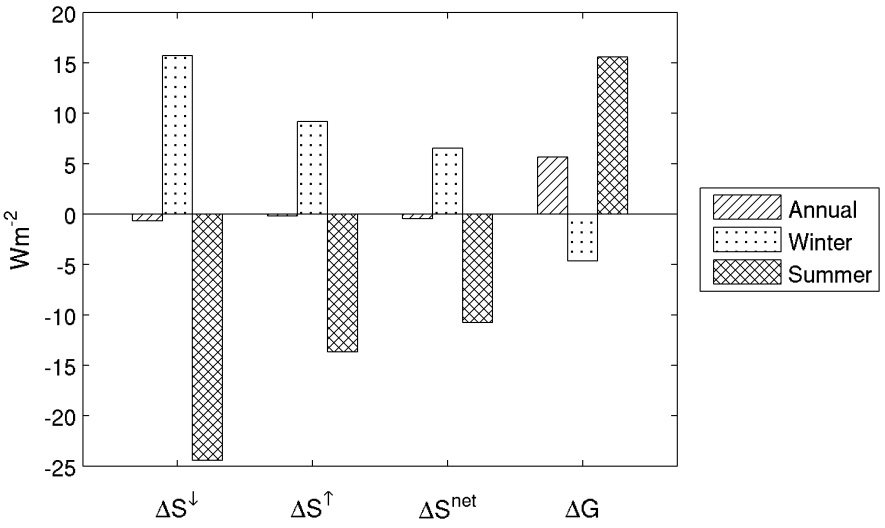

FIG. 9. The inter-hemispheric difference of downward shortwave radiation ($\Delta S^{\downarrow}$), upward shortwave radiation ($\Delta S^{\uparrow}$), and greenhouse trapping (ΔG) for annual mean (hatching), winter (dotted) and summer (crossing). Units are in Wm^{-2}.

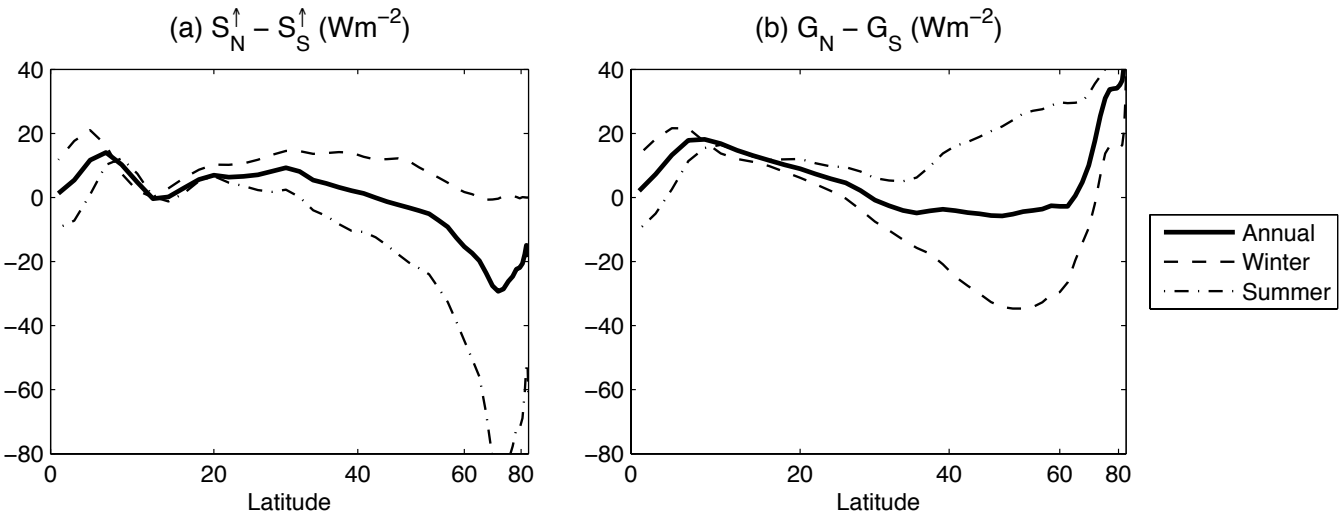

FIG. 10. The inter-hemispheric difference of (a) upward shortwave radiation ($\Delta S^{\uparrow}$), and (b) greenhouse trapping (ΔG) as a function of latitude for annual mean (thick solid), winter (thin dashed) and summer (thin dash-dot). Units are in Wm^{-2}.

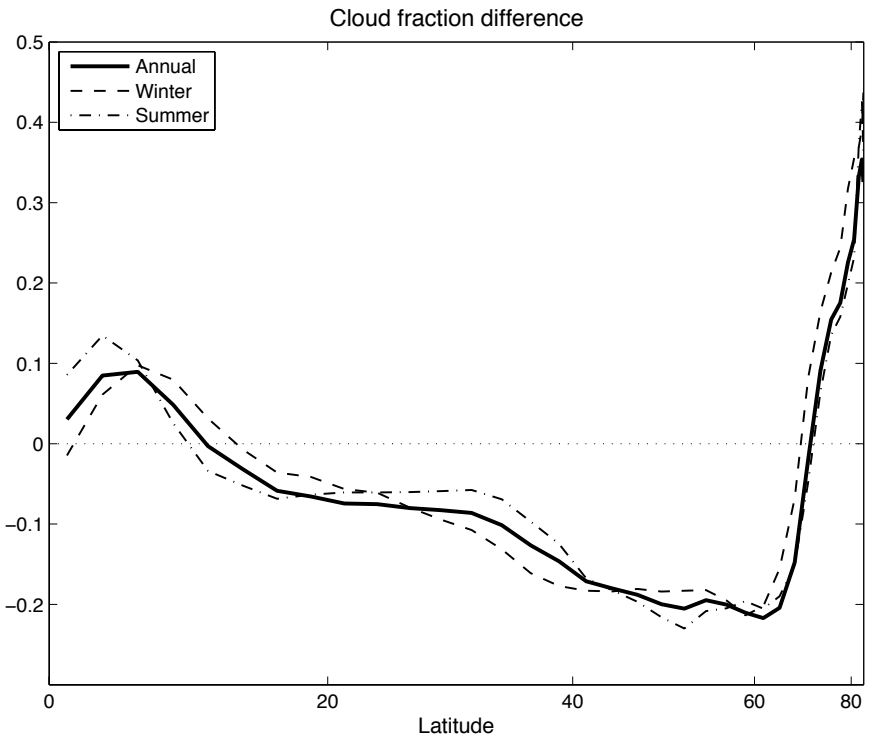

FIG. 11. The inter-hemispheric difference of cloud fraction with latitude for annual mean (thick solid), winter (thin dashed) and summer (thin dash-dot).

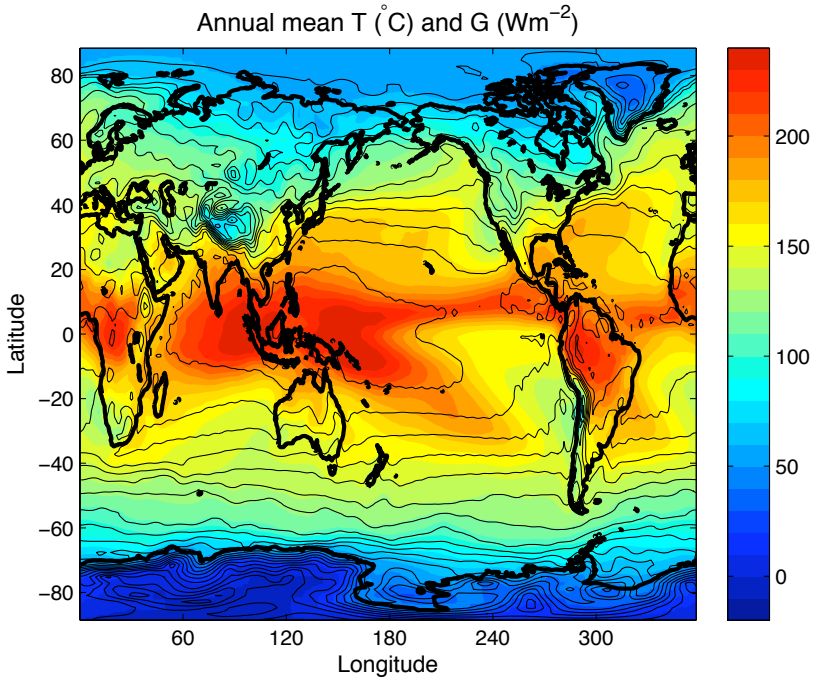

FIG. 12. The global map of annual mean surface temperature (in °C) in black contour and greenhouse trapping (in Wm^{-2}) in color shading. The contour interval is 4°C and shading interval is 10 Wm^{-2}.

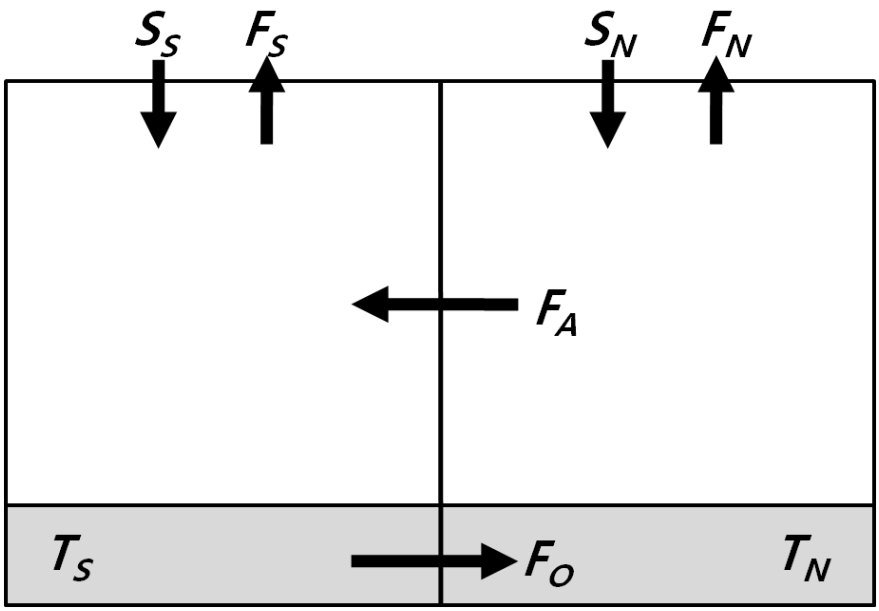

FIG. 13. The schematic figure for the box model based on energy budget. The net incoming shortwave radiation S is balanced by outgoing longwave radiation F, meridional energy transports by atmosphere F_A and ocean F_O. The model solves for surface temperature T. The subscripts N and S denote the hemispheric mean in the north and the south, respectively.

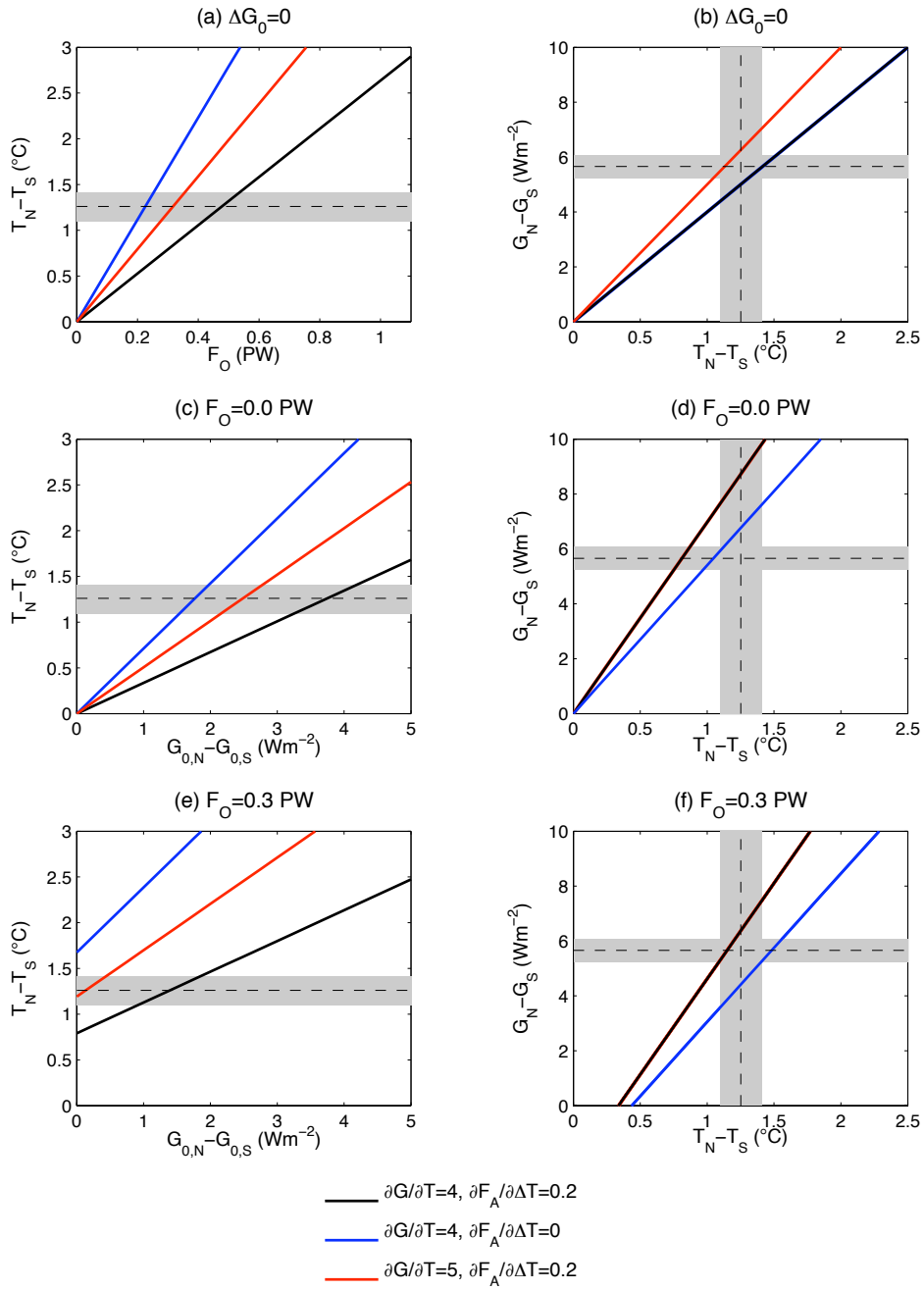

FIG. 14. Solutions from the box model: the inter-hemispheric difference of (a) surface temperature ($\Delta T = T_N - T_S$, in °C) as a function of prescribed oceanic transport F_O (in PW), and (b) greenhouse trapping ($\Delta G = G_N - G_S$, in Wm^{-2}) as a function of ΔT for the case with no basic state G difference (ΔG_0=0). (c,d) Same as (a,b) but as a function of $\Delta G_0 (= G_{0,N} - G_{0,S})$ for no oceanic transport (F_O=0). (e,f) Same as (c,d) but for the case with F_O=0.3PW. The reference state (black) is the solution with the most reasonable parameters, $\frac{\partial G}{\partial T}$=4.0$\mathrm{Wm}^{-2}\mathrm{K}^{-1}$ and $\frac{\partial F_A}{\partial \Delta T}$=0.20$\mathrm{Wm}^{-2}\mathrm{K}^{-1}$. Blue is the case with no cross-equatorial atmospheric heat transport $\frac{\partial F_A}{\partial \Delta T}$=0 and red is with stronger greenhouse trapping $\frac{\partial G}{\partial T}$=5.0$\mathrm{Wm}^{-2}\mathrm{K}^{-1}$. Black dashed lines denotes the annual mean values, and the gray shading denotes the one standard deviation of observed ΔT and ΔG.

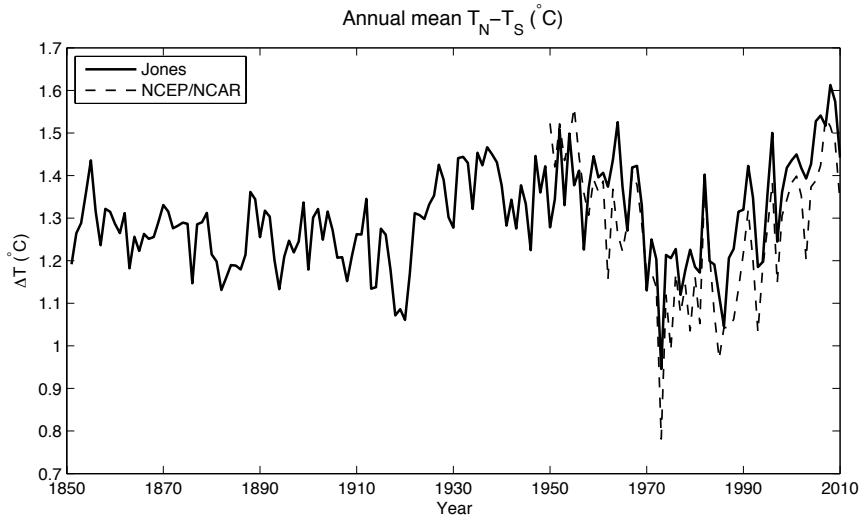

FIG. 15. The annual-mean inter-hemispheric temperature difference ($\Delta T = T_N - T_S$) in °C from 1850 to 2010 using the Jones et al. (1999) data (solid) and that from 1949 to 2010 using NCEP/NCAR reanalysis (dashed).